



On Damage Detection System Information for Structural Systems

Sebastian Thöns, Michael Döhler & Lijia Long

To cite this article: Sebastian Thöns, Michael Döhler & Lijia Long (2018) On Damage Detection System Information for Structural Systems, Structural Engineering International, 28:3, 255-268, DOI: [10.1080/10168664.2018.1459222](https://doi.org/10.1080/10168664.2018.1459222)

To link to this article: <https://doi.org/10.1080/10168664.2018.1459222>



Published online: 18 Jul 2018.



Submit your article to this journal [↗](#)



Article views: 74



View Crossmark data [↗](#)

On Damage Detection System Information for Structural Systems

Sebastian Thöns , Associate Professor, Department of Civil Engineering, Technical University of Denmark, Lyngby, Denmark and Department 7 Safety of Structures, BAM Federal Institute for Materials Research and Testing, Berlin, Germany; **Michael Döhler**, Research Scientist, Inria/IFSTTAR, Rennes, France; **Lijia Long**, PhD Student, Department 7 Safety of Structures, BAM Federal Institute for Materials Research and Testing, Berlin, Germany. Contact: sebt@byg.dtu.dk
DOI: 10.1080/10168664.2018.1459222

Abstract

Damage detection systems (DDSs) provide information on the integrity of structural systems in contrast to local information from inspections or non-destructive testing (NDT) techniques. In this paper, an approach is developed that utilizes DDS information to update structural system reliability and integrate this information into risk and decision analyses. The approach includes a novel performance modelling of DDSs accounting for the structural and measurement system characteristics, the damage detection algorithm (DDA) precision including type I and II errors. This DDS performance modelling provides the basis for DDS comparison and assessment in conjunction with the structural system performance including the damage and failure state dependencies. For updating of the structural system reliability, an approach is developed based on Bayesian updating facilitating the use of DDS information on structural system level and thus for a structural system risk analysis. The structural system risk analysis encompasses the static, dynamic, deterioration, reliability and consequence models, which provide the basis for calculating the direct risks due to component failure and the indirect risks due to system failure. Two case studies with the developed approach demonstrate a potential risk reduction and a high Value of DDS Information.

Keywords: damage detection; value of information; structural systems; damage detection uncertainty modelling, structural system updating.

Introduction

Damage detection systems (DDSs) provide information about the integrity and performance of structural systems. The performance of a structural system is characterized by its safety, i.e. the system reliability and risks, and its functionality namely the associated expected benefits and costs. Structural system reliability is generally modelled with failure and damage mechanisms that are based on static and dynamic system behaviour. These mechanisms generally have a statistical dependence caused by common influencing factors such as environmental conditions, production and construction processes and material characteristics.¹⁻³

Damage detection information is characterized by providing an indication of damage of a structural system subjected to a finite precision.⁴ The damage detection information provided by a measurement system and a damage detection algorithm (DDA) refers to a change in the

structural system characteristics in relation to a reference state of the structural system.^{5,6} Damage detection information thus accounts for the dependencies in the entire structural system.

Both structural system performance models and DDAs have progressed significantly but separately in the scientific literature in recent decades.^{5,7-12} However, it has been demonstrated that structural system identification based on response measurements can be combined with the updating of structural reliability and that such information can contribute to the accuracy of the structural condition and thus to structural safety.¹³

This paper thus focuses on: (a) explicitly modelling the characteristics of a structural system and its DDS, including the costs, consequences and functionalities, (b) utilizing the DDS for updating the structural system reliability, and (c) identifying the conditions under which DDS information may have a high value by utilizing

Bayesian decision analysis. The developed approaches are elaborated with two case studies, namely (1) an example focusing on how the structural system reliability can be updated and how a risk reduction can be achieved and (2) a case study containing a Value of DDS Information analysis of a bridge girder under high degradation.

Structural Performance Modelling, Inspection and Damage Detection Performance Modelling

Structural System Performance and Risk Modelling

Structural system reliability and risk are described by means of structural system theory, which is based on the probabilistic mechanical behaviour of the system in conjunction with its loading, resistance and deterioration models and the quantification of the system risks and utilities in conjunction with a consequence model.

Structural failure can be caused by an extreme static or dynamic loading of the system and/or its components. An extreme structural system loading implies a high statistical dependence of the component loadings. The dependence of the component resistances is governed by the production processes (e.g. section properties and material parameters) and the construction process (e.g. imperfections) of the structure.¹ Deterioration may cause damage to the structural system and can affect the entire system or occur at different locations and in different time periods, depending on the material and the nature of the damage mechanism. The spatial and componential dependence of damage mechanisms can thus vary significantly, such as for example in the fatigue of steel structures.¹⁴ The failure of a structural system and/or its components

caused by damage mechanisms thus rely on the structural system characteristics and the loading, resistance and damage mechanism dependencies.⁹

The performance of a structural system both in regard to system failure and system damage can be described with logical systems, Daniels systems and Bayesian networks.^{7,15,16} In general, the probability $P(F_S)$ of a structural system failure is calculated by integrating the joint probability density over the space of the system failure Ω_{F_S} :

$$P(F_S) = \int_{\Omega_{F_S}} f_X(\mathbf{x}) d\mathbf{X} \quad (1)$$

where the system failure space Ω_{F_S} is defined with limit state functions dependent on the vector of random variables \mathbf{X} . The structural risks can then be calculated with the n_c component and system probabilities of failure ($P(F_i)$ and $P(F_S)$) and the consequences of component and system failure (C_c and C_S). The risk may be classified into direct risk due to component failure and indirect risk due to system failure (R_D and R_{ID}) as follows¹⁷:

$$R = R_D + R_{ID} = \sum_{i=1}^{n_c} P(F_i) \cdot C_c + P(F_S) \cdot C_S \quad (2)$$

Damage Detection

Automatic damage detection methods in a structural health monitoring (SHM) context are based on the chosen measurement technology for the desired monitoring aim.^{4, 12} To illustrate the integration of damage detection information into the performance analysis of a structure, a vibration-based damage detection method is considered in the following.

Vibration monitoring is one of the best known and most well-developed techniques for long-term SHM and is recognized as an addition or alternative to visual inspections and the manual performance of local non-destructive testing (NDT).^{4,5,18,19} The rationale is that damage has an effect on the structural stiffness, and thus on the modal parameters (modal frequencies, damping ratios and mode shapes) which characterize the dynamics of the structure. A network of vibration

sensors (usually accelerometers) is attached to the structure to continuously measure the structural vibration responses to ambient excitation like wind, traffic, waves and other forces. Changes in the measured signals with respect to the dynamic characteristics of the structure then indicate the damage that these forces might have caused. Since changes in environmental conditions (such as temperature fluctuations) also lead to changes in the signals, they must be accounted for.^{20,21}

Methods for vibration-based damage detection compare the measurement data from the (healthy) reference state of the structure with data from the current, potentially damaged state, and an alarm is raised if the difference between both states exceeds a threshold. There are many methods for damage detection in this context.⁶ For example, a straightforward approach is to identify and directly compare the modal parameters from measurements of both the reference and current states.¹⁸ Other methods indirectly compare current measurements to a reference in a statistical difference measure without modal parameter identification. For instance, such methods include non-parametric change detection based on novelty detection,²² Kalman filter innovations,²³ methods from machine learning⁴ and many more. Also belonging to this class of methods, statistical subspace-based damage detection methods offer a flexible and well-founded theoretical framework that is used in this paper.^{10,11,19,24,25}

In the following, the subspace-based DDA is introduced as an example of a global automated damage detection method. With this method, vibration measurements from the current system are compared to a reference state in a subspace-based residual vector. In a hypothesis test, the uncertainties of the residual are taken into account and the respective χ^2 test statistic is compared to a threshold in order to decide whether or not the structure is damaged. Based on these properties, the χ^2 test statistic is considered as the damage indicator value (DIV) for damage monitoring.

Dynamic Structural System Model

The behaviour of the monitored structure is assumed to be described by the

following linear time-invariant dynamical system:

$$\mathbf{M}\ddot{\mathbf{z}}(t) + \mathbf{C}\dot{\mathbf{z}}(t) + \mathbf{K}\mathbf{z}(t) = \mathbf{v}_F(t) \quad (3)$$

where t denotes continuous time, \mathbf{M} , \mathbf{C} and $\mathbf{K} \in \mathbb{R}^{m \times m}$ are the mass, damping and stiffness matrices, the vector $\mathbf{z} \in \mathbb{R}^m$ collects the displacements of the m degrees of freedom of the structure and $\mathbf{v}_F(t)$ is the external force that is usually unmeasured for long-term monitoring. Observing the system described by Eq. (3) with a set of r acceleration sensors yields the following measurements:

$$\mathbf{y}(t) = \mathbf{L}\dot{\mathbf{z}}(t) + \mathbf{e}(t) \quad (4)$$

where $\mathbf{y} \in \mathbb{R}^r$ is the measurement vector, the matrix $\mathbf{L} \in \mathbb{R}^{r \times m}$ indicates the sensor locations and \mathbf{e} is the measurement noise.

Measurements are taken at discrete time instants $t = k\tau$, where k is an integer and τ is the time step. A sampling model consisting of Eq. (3) and Eq. (4) at the rate $1/\tau$ and transformed into a first-order system yields the following discrete-time state space model:

$$\begin{aligned} \mathbf{x}_{k+1} &= \mathbf{A}\mathbf{x}_k + \mathbf{v}_k \\ \mathbf{y}_k &= \mathbf{C}\mathbf{x}_k + \mathbf{w}_k \end{aligned} \quad (5)$$

where the states, outputs, state transition matrix and output matrix are as follows:

$$\begin{aligned} \mathbf{x}_k &= \begin{bmatrix} \mathbf{z}(k\tau) \\ \dot{\mathbf{z}}(k\tau) \end{bmatrix}, \\ \mathbf{y}_k &= \mathbf{y}(k\tau), \\ \mathbf{A} &= \exp\left(\begin{bmatrix} 0 & \mathbf{I} \\ -\mathbf{M}^{-1}\mathbf{K} & -\mathbf{M}^{-1}\mathbf{C} \end{bmatrix} \tau\right), \\ \mathbf{C} &= \mathbf{L} \begin{bmatrix} -\mathbf{M}^{-1}\mathbf{K} & -\mathbf{M}^{-1}\mathbf{C} \end{bmatrix} \end{aligned} \quad (6)$$

respectively and the appropriate state noise and output noise terms are \mathbf{v}_k and \mathbf{w}_k , respectively. The state noise is related to the unmeasured external force \mathbf{v}_F , while the output noise depends on both \mathbf{v}_F and the measured noise \mathbf{e} . Both noise terms are assumed to be stationary white noise for the theoretical outline of the damage detection method. While this assumption seems to be restrictive in real-world

applications on civil structures where the ambient excitation may be modelled by non-stationary and coloured noise, some robustness of the damage detection method to these conditions has been shown,¹⁰ which is supported by several case studies on structures in operation.¹⁹ The theoretical system order of the system in Eq. (5) is the dimension of the states $n = 2m$. Note that the above modelling is not only valid for acceleration measurements as in Eq. (4) but generalizable to displacement and velocity measurements.

The modal parameters of the model in Eq. (3) and Eq. (4)—namely the natural frequencies, damping ratios and observed mode shapes—are equivalently found in the system matrices (A, C) of the model in Eq. (5). Damage in the monitored system will correspond to changes in the matrices \mathbf{M} , \mathbf{C} and \mathbf{K} in Eq. (3), for example a loss of mass or loss of stiffness, and thus affect the system matrices (A, C) and the modal parameters. Hence, damage that occurs in the model in Eq. (3) can equivalently be detected as changes in the modal properties related to the system matrices (A, C) of Eq. (5).

Based on the measurements y_k of the monitored system from a reference and a possibly damaged state, a residual vector is defined based on subspace properties without identifying the system matrices (A, C) , as outlined in the following sections.

Subspace Properties

From the measurement data $\{y_k\}_{k=1, \dots, N}$, the correlations $R_i = \frac{1}{N} \sum_{k=1}^N y_k y_{k-i}^T$ are computed for $i = 1, \dots, p + q$, where p and q are chosen parameters (usually $p + 1 = q$) with $\min(pr, qr) \geq n$.²⁵ Then, they are filled into a block Hankel matrix:

$$\mathcal{H} = \begin{pmatrix} R_1 & R_2 & \dots & R_q \\ R_2 & R_3 & \dots & R_{q+1} \\ \vdots & \vdots & \ddots & \vdots \\ R_{p+1} & R_{p+2} & \dots & R_{p+q} \end{pmatrix} \quad (7)$$

This matrix possesses the factorization

property $\mathcal{H} = \mathcal{O} \mathcal{C}$, with the observability matrix:

$$\mathcal{O} = \begin{bmatrix} C \\ CA \\ \vdots \\ CA^{p+1} \end{bmatrix} \quad (8)$$

and the controllability matrix \mathcal{C} . Matrix \mathcal{O} can be obtained from a singular value decomposition (SVD) of \mathcal{H} , truncated at the model order n , as:

$$\begin{aligned} \mathcal{H} &= U \Delta V^T \\ &= (U_1 \ U_0) \begin{pmatrix} \Delta_1 & \\ & \Delta_0 \end{pmatrix} V^T, \quad (9) \\ \mathcal{O} &= U_1 \Delta_1^{1/2} \end{aligned}$$

Note that the truncated singular values correspond to noise and are usually small, namely $\Delta_0 \approx 0$.

Once \mathcal{O} is obtained from Eq. (7) and Eq. (9), the system matrices (A, C) can be extracted from Eq. (8) for subspace-based system identification,^{26,27} from which the modal parameters can be obtained. Instead of carrying out this system identification step, however, the subspace properties are used for the definition of a damage detection residual and a subsequent damage detection test.

Damage Detection Residual and Test

Let \mathcal{H}^0 be a Hankel matrix (Eq. (7)) filled with data from a (healthy) reference state, and let its SVD in Eq. (9) be given. Define its left null space matrix S , obtained as $S = U_0$ in Eq. (9), such that $S^T \mathcal{H}^0 \approx 0$.

Now, let the new measurements $\{y_k\}_{k=1, \dots, N}$ from an unknown state of the system be given, from which a new Hankel matrix \mathcal{H} is computed. If the data comes from the system in the reference state then S is still a null space of \mathcal{H} since the modal parameters and thus the matrices (A, C) (up to a change of basis) are unchanged. Thus, $S^T \mathcal{H} \approx 0$ is a characteristic property of the system in the reference state.

However, if the system is damaged, the modal properties related to the matrices (A, C) and thus to \mathcal{O} in Eq. (8) change, and the mean of the product $S^T \mathcal{H}$ deviates from 0. Note that the matrix \mathcal{H} is computed from data and does not depend on the state basis of the matrices (A, C) .

These properties lead to the definition of the residual vector^{10,11,24}:

$$\zeta = \sqrt{N} \text{vec}(S^T \mathcal{H}) \quad (10)$$

where N is the number of samples from which \mathcal{H} is computed. This residual vector is asymptotically Gaussian (for a large N) with a zero mean in the reference state and a non-zero mean in the damaged state.¹⁰ Thus, a change in the system corresponds to a deviation from 0 in the mean value of the residual vector. The corresponding hypothesis test (for a decision between \mathbf{H}_0 : the system is in the reference state and \mathbf{H}_1 : the system is in the damaged state) leads to the following test statistic:

$$d = \zeta^T \Sigma^{-1} \zeta \quad (11)$$

where $\Sigma = \mathbf{E}(\zeta \zeta^T)$ is the residual covariance matrix. An estimate of Σ is the sample covariance that is computed on several realizations of the residual using measurement data in the reference state. Due to the distribution properties of the residual, the test statistic (Eq. (11)) is asymptotically χ^2 distributed with a non-centrality parameter in the damaged state.^{10,11} To decide whether or not the monitored structure is damaged, the test statistic is compared to a threshold. Based on realizations of the test statistic in the reference state, the threshold is typically defined to reduce the probability of false alarms (type I errors) occurring to below a chosen level, while keeping in mind that a lower probability of false alarms (lower type I errors) also leads to a lower probability of indications of small amounts of damage (higher type II errors) being detected. In practice, a trade-off between both needs to be made. In the following, the event of *indication* is defined as the detection of damage, namely when the test statistic exceeds the threshold. Note that the terms *probability of indication* and *probability of detection* can be used equivalently. Thanks to the previous properties, the test statistic (Eq. (11)) is considered as the DIV in the following analysis.

Note that Eq. (11) is the non-parametric version of the damage detection test.^{11,20} A detailed description of the statistical framework and more theoretical and computational insight of this method are given in Refs. [10, 11, 25].

Updating the Structural System Reliability with Damage Detection Information

The approach to update the structural system reliability and risks is presented at the end of this section, based on an outline of the inspection and measurement performance modelling and the DDS performance modelling detailed below.

Inspection and Measurement Performance Modelling

Inspection and measurement performance can be modelled based on the approaches of NDT, non-destructive evaluation (NDE) and non-destructive inspection (NDI) reliability modelling.^{28–30} In the following, methods of NDT modelling are reviewed and a consistent performance model is introduced to provide the basis for the DDS performance assessment.

The NDT reliability calculation is based upon modelling or measuring the signal given damage and the noise (given no damage) of the NDT hardware. Assume that an indication event I is defined when the signal exceeds a predefined threshold t_D . Depending on this threshold, the conditional probabilities of the indication event are calculated with the signal s and the noise s_0 , where n_D component damage states of a structural component are modelled as discrete and disjoint, that is $\psi_j, j = 1, \dots, n_D$, and ψ_0 is defined as the undamaged state. The probability of the complementary events indication (I) and no-indication (\bar{I}) for a component damage state ψ_j , namely $P(I|\psi_j)$ and $P(\bar{I}|\psi_j)$, respectively, are determined by integrating the probability density f of the signal:

$$P(\bar{I}|\psi_j) = \int_{-\infty}^{t_D} f(s|\psi_j) ds \quad (12)$$

$$P(I|\psi_j) = \int_{t_D}^{\infty} f(s|\psi_j) ds \quad (13)$$

The probability of indication and no-indication given no damage ($P(I|\psi_0)$ and $P(\bar{I}|\psi_0)$) are calculated by integrating the noise s_0 :

$$P(\bar{I}|\psi_0) = \int_{-\infty}^{t_D} f(s_0|\psi_0) ds_0 \quad (14)$$

$$P(I|\psi_0) = \int_{t_D}^{\infty} f(s_0|\psi_0) ds_0 \quad (15)$$

Note that these probabilities are given for an upper boundary threshold t_D , namely damage is indicated when the signal exceeds this threshold, but they can still easily be generalized to the case of a lower boundary or two-sided thresholds, for example. The probability densities f of the noise and the signal can be determined with inter-laboratory tests performed independently several times (so-called round robin tests) which imply a frequentistic basis,^{28–30} or analytically and numerically by simulating the NDT process.^{31,32}

With the above four equations, the probability of indication, the probability of a false alarm and the receiver operating characteristics (ROCs) are defined. An example of a probability of indication (or probability of detection) plot covering the probability of indication given no damage, ψ_0 , and different damage states, $\psi_j, j = 1, \dots, n_D$, is depicted in Fig. 1 for a constant threshold. Please note that the diagram contains a (non-zero) probability of indication given no damage (ψ_0), which is also referred to as the probability of false alarm.

The probability of a false alarm is defined as the probability of indication given an undamaged structural component $P(I|\psi_0)$.³³ It is understood that the probability of a false alarm is caused by noise, since damage is absent by definition. Data normalizing efforts usually aim at reducing or averaging out the noise.¹² The ROC is a plot of the probability of indication, $P(I|\psi_i)$, against the probability of a false alarm, $P(I|\psi_0)$, for a particular damage state ψ_i but varying the threshold t_D .

The approach of NDT reliability modelling as outlined above has recently been applied on a component level to modelling DDA probabilities of indication, for example with the purpose of assessing their quality.^{33–35} For this aim the signal is defined as the DIV in the damaged state and the noise is defined as the DIV produced by the DDA in the reference state, that is the state where the structural system is undamaged. With these definitions, the probabilities of indication and no-indication given no damage and damage can be calculated as per Eq. (12), Eq. (13), Eq. (14) and Eq. (15).

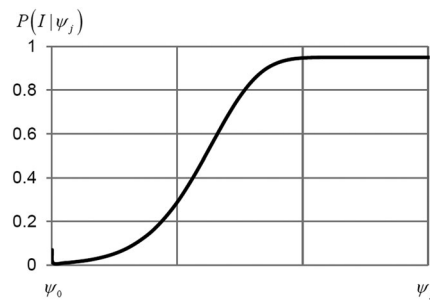


Fig. 1: Exemplary probability of indication curve for one component

Damage Detection System Performance Modelling

In order to apply the above NDT reliability modelling to DDS, the following important characteristics of the DDS information have to be taken into account:

1. DDS information is provided by algorithms processing measurement system signals.
2. The measurement system is attached to a structural system.
3. The DDS is operated by humans.

Regarding the first characteristic, the DIV is usually a random variable due to the statistical signal processing of finite measurement data. Its statistical properties are influenced by various factors, including data length, measurement uncertainties and uncertain environmental conditions like the properties of ambient excitation. Regarding the second characteristic, the DIV for damage detection is a value that indicates changes in the entire structural system, meaning that damage in each of the components can have a different influence on the DIV. Hence, the damage states of the system need to be defined in conjunction with the structural components and the structural system performance. DDS information is also subjected to human errors, as per the third characteristic, which need to be taken into consideration.³¹

These major DDS characteristics are incorporated as follows. The structural system is discretized into n_c components with discrete damage states. For example, these components may correspond to the elements of a finite-element method (FEM) model of the structure. Let each of the components $i \in \{1, \dots, n_c\}$ have $(n_D + 1)$ possible states, namely an undamaged state and n_D damage states. For simplicity of notation, an equal number of n_D

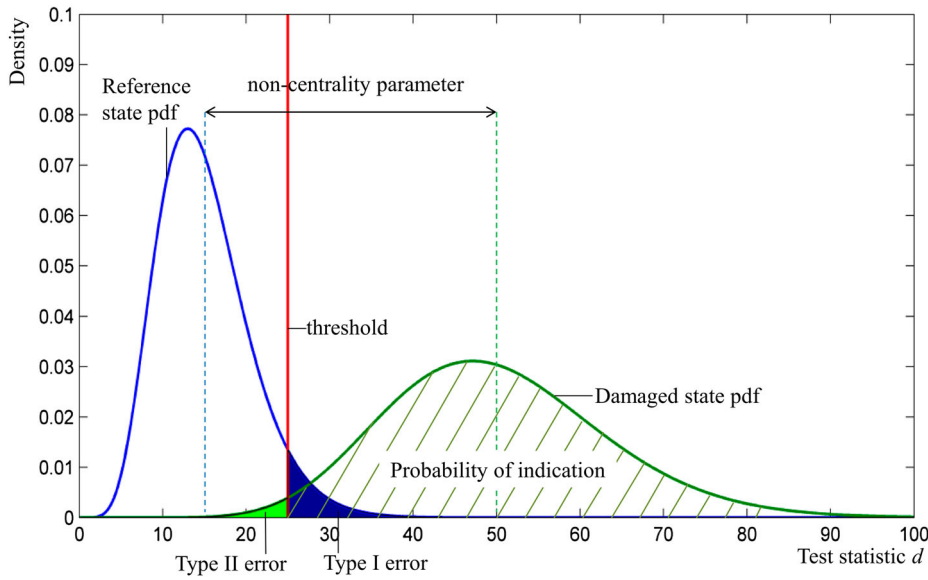


Fig. 2: Scheme of probability density functions of the damage detection test statistic d in the reference and in a damaged state

damage states is assumed for each component, which can be easily generalized. The respective states are denoted by ψ_{i,j_i} , where $j_i = 0$ for the undamaged state and $j_i = 1, \dots, n_D$ for the damage states of component i . Then, a full discretization of the structural system states contains the possible combinations of all of these states, amounting to $(n_D + 1)^{n_c} - 1$ system damage states plus the undamaged state. Each of these states then corresponds to a particular set of matrices describing the monitored system in Eq. (3), where the damage states correspond to modifications of the matrices \mathbf{M} , \mathbf{C} and \mathbf{K} . The system damage space Ψ^{n_c} is then defined by the vectors $\Psi_{\mathbf{j}} = \{\psi_{1,j_1}, \dots, \psi_{n_c,j_{n_c}}\}$, where $\mathbf{j} = \{j_1, \dots, j_{n_c}\}$. Note that $\Psi_0 = \{\psi_{1,0}, \dots, \psi_{n_c,0}\}$ denotes the undamaged state.

Let the DIV $d_{\mathbf{j}}$ be given, which is obtained for any of these states $\Psi_{\mathbf{j}}$, whether the undamaged state or a damage state, and let its probability density function be given by $f(d_{\mathbf{j}}|\Psi_{\mathbf{j}})$. The probabilities of indication and no-indication given a damaged structural system can then be calculated by integrating the probability densities of the DIV, namely:

$$P(\bar{I}_S|\Psi_{\mathbf{j}}) = \int_{-\infty}^{t_{S,D}} \int f(d_{\mathbf{j}}|\Psi_{\mathbf{j}}) dd_{\mathbf{j}} \quad (16)$$

$$P(I_S|\Psi_{\mathbf{j}}) = \int_{t_{S,D}}^{\infty} f(d_{\mathbf{j}}|\Psi_{\mathbf{j}}) dd_{\mathbf{j}} \quad (17)$$

Note that the probability of no-indication in Eq. (16) is a *type II error*. In the considered damage detection method, the DIV is χ^2 distributed (Eq. (11)). Thus, the probability density function f corresponds to the classical χ^2 distribution in the undamaged state, and to a non-central χ^2 distribution in the damaged state. An example of the distributions of the DIVs d_0 and $d_{\mathbf{j}}$ with $\mathbf{j} \neq 0$ are given in Fig. 2. The threshold—which is set up from test values in the reference state for a given type I error—is depicted, along with the type II error

(corresponding to Eq. (16)) and the probability of indication (corresponding to Eq. (17)).

The distribution of the DIV that is required to evaluate the probabilities in Eq. (16) and Eq. (17) may be obtained in two different ways. First, it can be derived from the theoretical properties of the DDA, the damage state and (assumptions on the) statistical properties of the measurement data. For the presented damage detection method, the distribution of the DIV is known depending on a damage parameterization.^{10, 36} In this case, the damage parameters can be obtained from an FEM model of the structure. Second, the distribution of the DIV may be obtained numerically from Monte Carlo simulations, where measurement data is simulated in the respective damage states. This second option is particularly useful when the theoretical DIV distribution is unknown or difficult to evaluate—however, it comes with an additional computational burden.

An example of the probability of indication computed with Eq. (17) is depicted in Fig. 3 for a system with two components, building upon the subspace-based DDA presented in the previous section. It is observed that the probability of indication of a damage state $P(I_S|\{\psi_{1,j_1}, \psi_{2,j_2}\})$ with $\{j_1 \neq 0, j_2 \neq 0\}$ is higher than for component damage states $(P(I_S|\{\psi_{1,j_1}, \psi_{2,j_2}\})$ with $\{j_1 = 0, j_2 \neq 0\}$ or $\{j_1 \neq 0, j_2 = 0\}$).

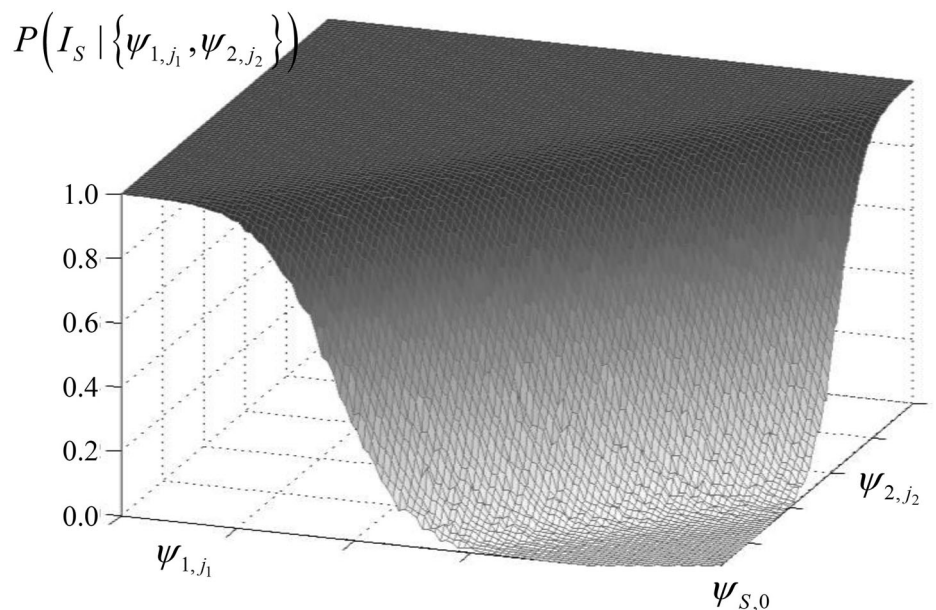


Fig. 3: Example of a probability of indication curve for a system consisting of two components dependent on the component damage state $\psi_{1,j_1=1} \dots \psi_{1,j_1=n_D}$ and $\psi_{2,j_2=1} \dots \psi_{2,j_2=n_D}$ and $\psi_{S,0} = \{\psi_{1,0}, \psi_{2,0}\}$

Note that the determination of the probability of indication for a structural system accounting for all possible damage states may be a non-trivial task, as the number of damage states increases exponentially with an increasing number of components. One approach to circumvent this challenge is to infer the probability of indication by the properties of the DDA.³⁶

Structural System Performance Updating

The approach to structural reliability updating has undergone several developments in recent decades. The early and comprehensive work in Ref. [37] contains a framework for structural reliability updating that includes inspection and monitoring information and accounts for measurement uncertainties. Recently, approaches have emerged for modelling and updating the system deterioration state of structures that take into account the aspect of spatial correlation among element deterioration.^{8,38–41} However, the impact of deterioration on structural system reliability is seldom included in these works, and only very recent studies can be found which integrate deterioration into structural system reliability.^{42–44} These approaches have in common that only local information provided by inspections for example is utilized, that is these approaches do not cover the characteristics of the DDS information, namely the dependency of the measurement system and structural system and that DDS may be able to detect correlated component damage states with a higher probability.

The formulation of the structural performance and the DDS performance on a system level as presented above facilitates the updating of the structural system reliability. The probability of structural system failure subjected to the system damage $\Psi^{nc}(t_S)$ given the DDS information of no-indication, $P(F_S(t_S)|\Psi^{nc}(t_S)|\bar{I}_S)$, can be determined utilizing Bayesian updating for any point in time during the service life t_S as follows:

$$\begin{aligned} & P(F_S(t_S)|\Psi^{nc}(t_S)|\bar{I}_S) \\ &= \frac{P(\bar{I}_S|F_S(t_S)|\Psi^{nc}(t_S))P(F_S(t_S)|\Psi^{nc}(t_S))}{P(\bar{I}_S|\Psi^{nc}(t_S))} \\ &= \frac{P(F_S(t_S)|\Psi^{nc}(t_S) \cap \bar{I}_S|\Psi^{nc}(t_S))}{P(\bar{I}_S|\Psi^{nc}(t_S))} \end{aligned} \quad (18)$$

It should be noted that the DDS information itself refers to a point or period in time that is neglected here for clarity.

The probability of no-indication $P(\bar{I}_S|\Psi^{nc}(t_S))$ given the system damage state can be calculated based on the developed approach for the DDS performance calculation (Eq. (17)). Following on from this,⁴⁵ the marginal probability of no-indication is calculated by integrating the product of the conditional probability of no-indication $(1 - P(I_S|\Psi^{nc}))$ and the joint probability density of the system damage space $f_{\Psi^{nc}}(\Psi^{nc})$ over the damage state spaces. The integration is performed over the space $\Omega_{\bar{I}_S}$, which is defined with the limit state function $g_{\bar{I}_S}$ as the difference between the probability of indication $P(I_S|\Psi^{nc})$ and a uniformly distributed random variable u , holding:

$$P(\bar{I}_S) = \int_{\Omega_{\bar{I}_S}} (1 - P(I_S|\Psi^{nc})) f_{\Psi^{nc}}(\Psi^{nc}) d\Psi^{nc} \quad (19)$$

with

$$\Omega_{\bar{I}_S} = \{g_{\bar{I}_S} = P(I_S|\Psi^{nc}) - u\}$$

To illustrate the characteristics of DDS information, the risk-quantification model is further detailed, which accounts for the direct and indirect risks (R^{DDS} and R_{ID}^{DDS}) at time t_S with DDS information and yields the following:

$$\begin{aligned} R^{DDS}(t_S) &= R_D(t_S) + R_{ID}^{DDS}(t_S) \\ &= \sum_{i=1}^{n_c} P(F_i(t_S)) \cdot C_c \\ &\quad + P(F_S(t_S)|\bar{I}_S(t_S)) \cdot C_S \end{aligned} \quad (20)$$

Only the indirect risks are updated due to the system characteristics of the DDS information. In contrast, the direct risks are updated by NDT information, as these refer to local indications of damage. It may be argued that DDS information may apply to both the structural system and its components. However, the updating of the component performance presupposes damage localization, which is outside the scope of this paper.

A risk reduction $\Delta R(t_S)$ can be quantified by subtracting the risk given by the DDS information and accounting for the expected SHM costs $E[C_{DDS}(t_S)]$

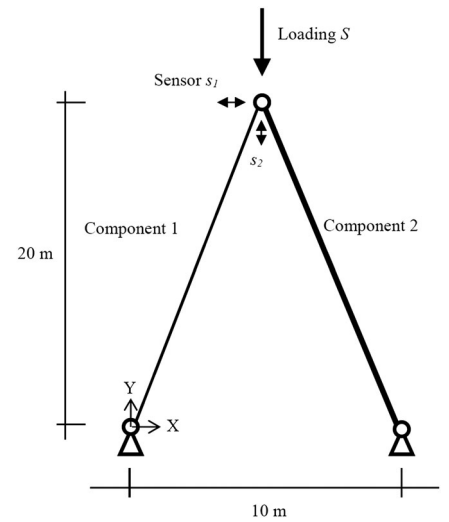


Fig. 4: Structural system with sensor locations

from the total risk without DDS information, which leads to:

$$\Delta R(t_S) = R(t_S) - (R^{DDS}(t_S) + E[C_{DDS}(t_S)]) \quad (21)$$

Relative risk reduction relates the risk reduction to the total risks not utilizing DDS information as follows:

$$\frac{\Delta R(t_S)}{R(t_S)} = \frac{R(t_S) - (R^{DDS}(t_S) + E[C_{DDS}(t_S)])}{R(t_S)} \quad (22)$$

Example: Structural Risk Reduction with DDS Information for a Simplistic Structural System

To illustrate the developed approach, the effects of the structural system and DDS characteristics on structural reliability and risk are quantified. For clarity, a simplistic structural system subjected to deterioration consisting of two components and a DDS comprising two sensors and a subspace-based DDA (Fig. 4) are described, with the system's static, dynamic, deterioration, reliability and consequences characteristics defined as required and outlined in the previous sections.

The structural system properties are modelled with distributed component stiffness and mass subjected to a structural damping of 2% for each mode (Table 1). The system behaviour is calculated using the FEM. For each of the structural components, $n_D = 100$ damage states ψ_{1,j_1} and ψ_{2,j_2} are considered, corresponding to stiffness losses from 0 to 10%. The resulting

Parameter	Value
Mass per component	0.5
Stiffness of component 1: EA_1	1000
Stiffness of component 2: EA_2	2000
Damping ratio	2%

Table 1: Structural model properties

system damage states are $\psi_j = \{\psi_{1,j_1}, \psi_{2,j_2}\}$ for $j_1, j_2 = 1, \dots, n_D$.

Due to the absence of redundancy, the structural system reliability is modelled as a series system, yielding:

$$P(F_S) = P\left(\bigcup_{i=1}^{n_c=2} M_{R,i}R_i(t_S) - M_S S_i \leq 0\right) \quad (23)$$

The formulation contains the number of components $n_c = 2$ with the random variables component resistance R_i (dependent on the time t_S) and the system loading S , along with their associated model uncertainties $M_{R,i}$ and M_S , respectively. The time-dependent resistance $R_i(t_S)$ of the component i is modelled with the initial resistance $R_{i,0}$ and the time-dependent damage $D_i(t_S)$:

$$R_i(t) = R_{i,0}(1 - D_i(t_S)) \quad (24)$$

For clarity, the temporal dependence of the damage is neglected in what follows.

The structural reliability model is summarized in Tables 2 and 3. The system loading is represented with a Weibull distributed random variable S , which results by equilibrium in the component loading S_i . The loading and resistance model uncertainties and the

Random variables	Coefficient of correlation
Resistance ρ_{R_0}	0.5 (when not varied)
Damage ρ_D	0.5 (when not varied)

Table 3: Correlation model

resistance model are determined according to Ref. [1] as Lognormal distributed with a standard deviation of 10%. The component probability of failure is calibrated to $1 \cdot 10^{-3}$ (when not varied) by adjusting the mean of the component resistance in the undamaged state based on ISO 2394 (2015)² and the JCSS Probabilistic Model Code.¹ The correlation of the resistances and the deterioration are modelled with a coefficient of correlation of 0.5 when not varied.

The consequence model for the calculation of risk builds upon the generic normalized costs for component failure $C_c = 1.0$, the structural system failure $C_S = 100$ (e.g. see Ref. [17]) and the DDS, C_{DDS} , comprising the DDS investment (1.33×10^{-4} per channel), installation (1.33×10^{-4} per channel) and operation (1.33×10^{-4} per year) in accordance with Ref. [46].

The DDS is modelled with the acceleration sensors s_1 in the x -direction and s_2 in the y -direction, recording the responses y_k from the system laid out in Eq. (3), Eq. 4 and Eq. (5) using the subspace-based DDA described previously. Based on the dynamic structural system model, 1000 data sets of length $N = 10\,000$ at a sampling frequency of 50 Hz are simulated for each of the undamaged and damaged states for both sensors from white noise excitation.

The probabilities of indication $P(I_S|\psi_j)$ and $P(I_S|\psi_0)$ are determined for the considered DIV in Eq. (11) with the

threshold t_D corresponding to a 0.01 probability of a type I error (see also Fig. 2). The DDA takes into account the uncertainties related to the measurement data of finite length N , which is due to the unknown ambient excitation and the measurement noise. Human errors in the application and operation are accounted for by the multiplication of the probability of indication with a factor of 0.95.³¹

The probabilities of indication based on data from sensors s_1 and s_2 dependent on the system damage state defined as axial stiffness reduction are depicted in Fig. 5. It is observed that the probabilities of indication based on sensor s_2 are significantly higher, which is caused by the higher axial stiffness of the system in the y -direction and thus higher absolute stiffness changes due to the simulated damages. It is further observed that damage of similar size in both components can be detected with a higher probability than individual damage in one of the components.

The DDS information is utilized to update the structural system reliability of the deteriorated structural system. The correlation characteristics of the deteriorated structural system may vary significantly due to the component, the system and the deterioration characteristics (as identified previously). The updated reliabilities and risks are thus depicted dependent on the resistance and deterioration correlation to allow for more generality of the example.

The deteriorated series system before being updated by DDS information shows a slight decrease in the structural system failure probability for both increasing the deterioration and the resistance correlation ρ_{R_0} and ρ_D (Fig. 6). When utilizing the DDS information, the failure probability decreases and a higher decrease rate for the deterioration correlation is observed for sensors s_1 and s_2 . However, both effects are significantly more pronounced for sensor s_2 due to the higher probabilities of indication (Fig. 6). The higher decrease rate for the damage correlation in comparison to the resistance correlation is explained by the higher probability of indication for correlated instances of damage of the same size—namely the higher the system deterioration, the better the DDS performance.

Random variable	Distribution*	Mean	Standard deviation
Loading S	WBL	3.50	0.10
Model uncertainty M_S	LN	1.00	0.10
Component resistance in undamaged state $R_{0,i}$	LN	Calibrated	0.10
Model uncertainty $M_{R,i}$	LN	1.00	0.10
Damage D_i	N	0.07	0.03

* LN = Lognormal; N = Normal; WBL = Weibull.

Table 2: Structural reliability model

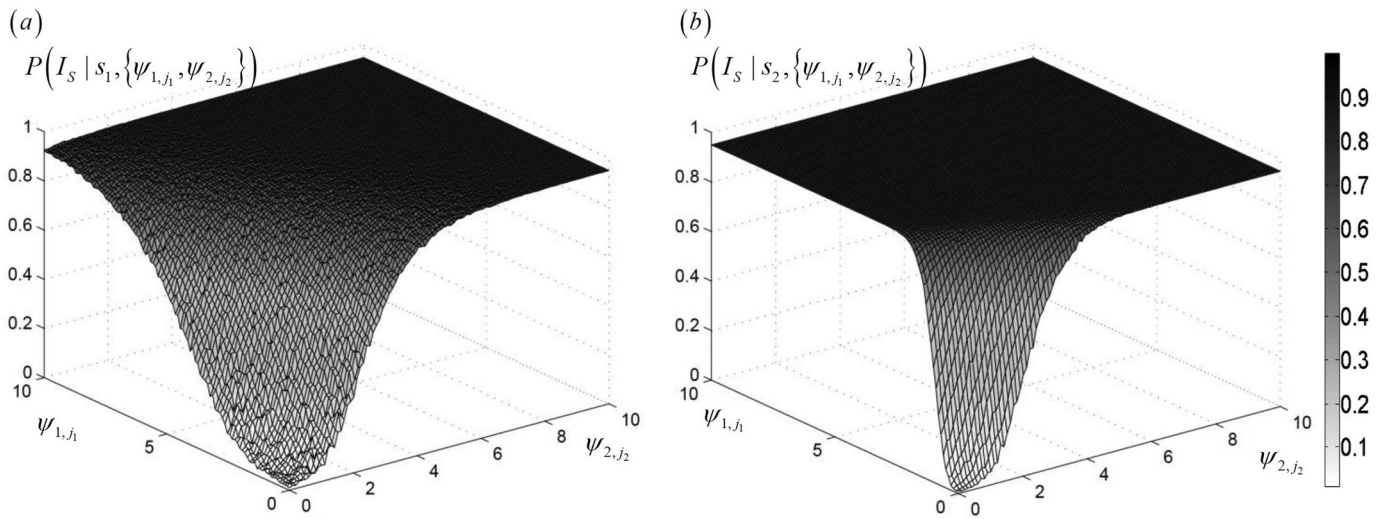


Fig. 5: Probability of indication dependent on the system damage states for: (a) sensor s_1 ; (b) sensor s_2

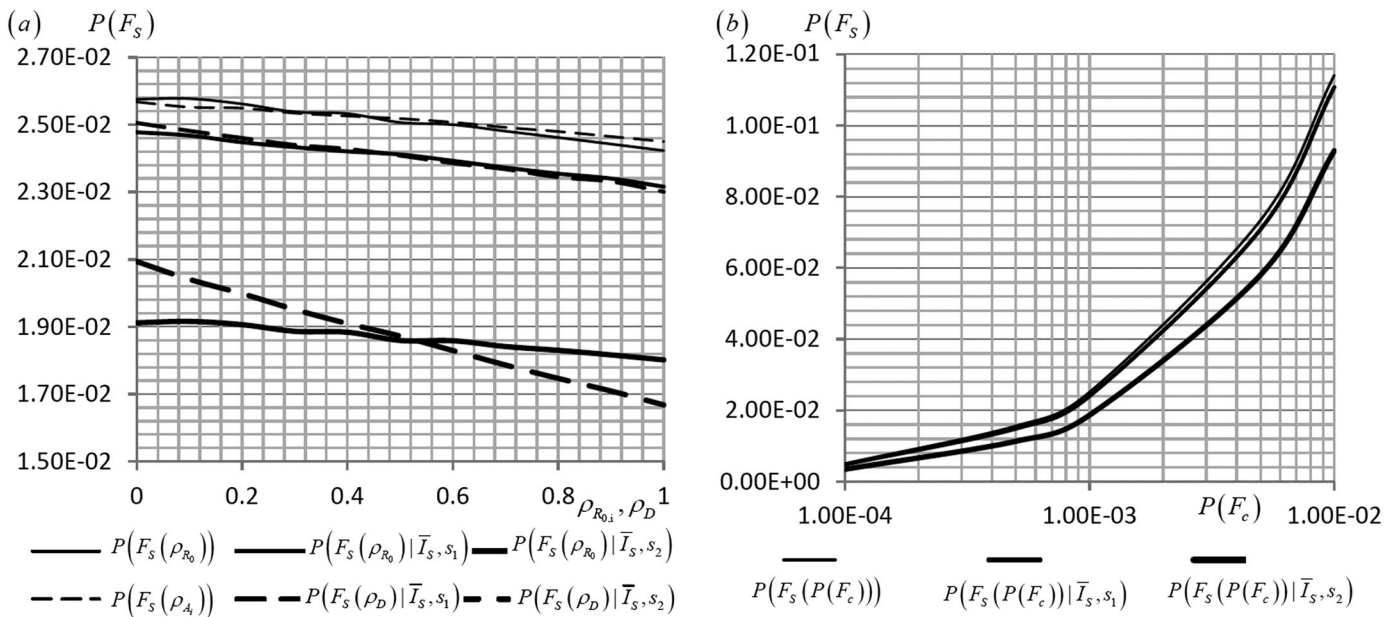


Fig. 6: Prior and posterior system probability of failure ($P(F_S)$ and $P(F_S|\bar{I}_S)$) for different sensor positions dependent on the damage and resistance correlation (a) and the probability of component failure (b)

An exponential dependency of the structural system failure probability on the component probability of failure is observed (Fig. 6b). The dependency is explained by the interdependency of the component failure and the system failure. The system failure probability is more reduced when using sensor s_2 due to the higher probability of indication of structural damage.

The risk reduction ΔR and the relative risk reduction $\Delta R/R$ according to Eq. (21) and Eq. (22) dependent on the damage and the resistance correlation are shown in Fig. 7. The risk reduction for both sensors is positive despite considering the expected SHM costs, which means that the expected SHM

costs are overcompensated for by the risk reduction due to the DDS information.

It is observed that sensor s_2 leads to a significantly higher risk reduction than sensor s_1 , which is caused by a higher reduction in the probability of system failure. The higher risk reduction decrease rate observed for the damage correlation is in line with the findings in Ref. [2].

The relative risk reduction relates the absolute risk reduction to the total risks without utilizing the DDS information and can thus be seen as a measure for the significance of the risk reduction. The risk reduction varies between 2.3 and 6.0% for

sensor s_1 and between 18.4 and 32.8% for sensor s_2 (Fig. 7b). The behaviour of the relative risk reduction dependent on the damage and the resistance correlation is very similar to the risk reduction, as the system failure probability varies linearly and to a limited extent.

A higher absolute risk reduction is observed for systems with a higher probability of component and thus system failure (Fig. 8a). This effect has also been observed for a ductile Daniels system with an SHM strategy of load monitoring.⁴⁴ However, the relative risk reduction (Fig. 8b) decreases, as the system risk increase rate is higher than the risk reduction rate.

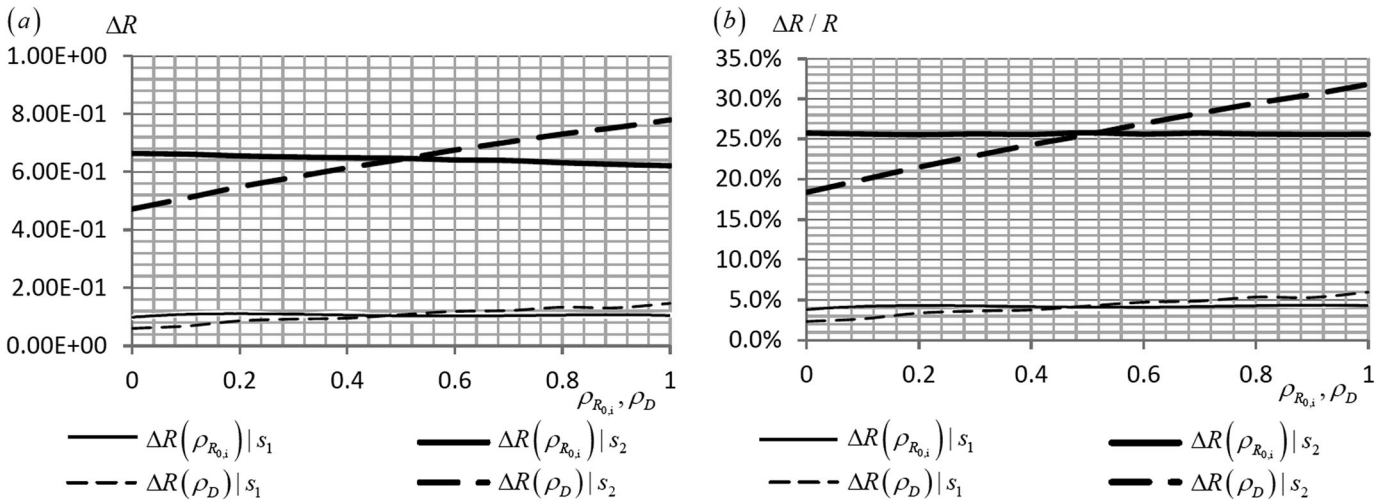


Fig. 7: Structural risk reduction dependent on the resistance and damage correlation for different sensor positions: (a) absolute risk reduction ΔR ; (b) relative risk reduction $\Delta R/R$

It has been demonstrated that a significantly higher uncertainty and risk reduction can be achieved with sensor s_2 . The performance of the sensor in the context of this study relies on more efficiently capturing the dynamic behaviour of the structural system, thus facilitating higher sensitivity and thus a higher probability of detecting small damages. For a further optimization of DDS, these characteristics and the interrelations of the structural and DDSs have to be considered.

Utility Gain Quantification for Damage Detection Information

The value of the damage detection information, namely the utility gain by applying DDSs, can be quantified based on the approach for the quantification of the value of the structural

health monitoring information² (V) as the difference between the life-cycle benefits B_1 and B_0 with and without the DDS strategy i :

$$V = B_1 - B_0 \quad (25)$$

The expected value of the life-cycle benefit B_0 is formulated as a prior decision analysis, that is the maximization of the expected benefits b_0 with the k_n action choices $\mathbf{a} = [a_1 \dots a_k \dots a_{k_n}]^T$ and the l_n structural performance uncertainties $\mathbf{X}_k = [X_1 \dots X_l \dots X_{l_n}]^T$:

$$B_0 = E_{X_{k,l}}[b_0(a_k^{*,0}, X_l)]$$

with

$$a_k^{*,0} = \arg \max_{a_k} (E_{X_{k,l}}[b_0(a_k, X_l)]) \quad (26)$$

Utilizing DDS strategies s_i , the expected value of the life-cycle benefit B_1 is calculated by additionally considering the j_n uncertain DDS information $\mathbf{I}_{s_i} = [I_{s_i,1} \dots I_{s_i,j} \dots I_{s_i,j_n}]^T$ with the extensive form of a pre-posterior decision analysis:

$$B_1 = E_{Z_{s_i,j}}[E''_{X_{k,l}}[b_i(s_i^*, I_{s_i,j}, a_k^{*,i}, X_l)]]$$

with

$$(s_i^*, a_k^{*,i}) = \arg \max_{s_i} E_{I_{s_i,j}}[\arg \max_{a_k} E''_{X_l}[b_i(s_i, I_{s_i,j}, a_k, X_l)]] \quad (27)$$

The calculation of the expected benefits necessitates explicit benefit, cost and risk models dependent on DDS strategies, its outcomes, the actions and the life-cycle performance. These models are exemplarily

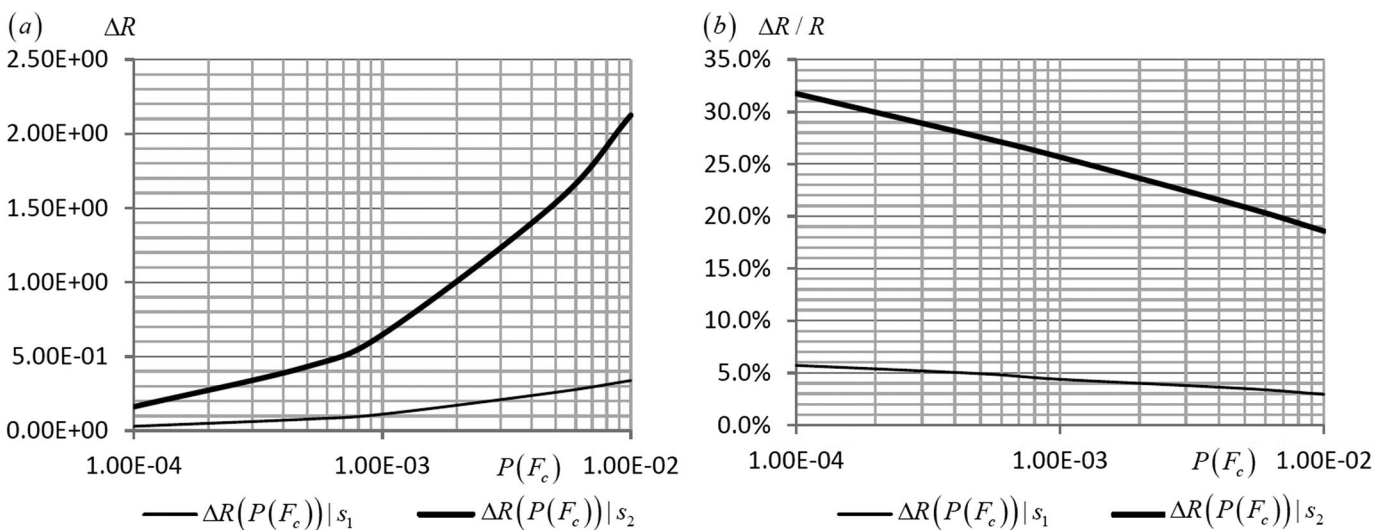


Fig. 8: Structural risk reduction dependent on the component probability of failure for different sensor positions: (a) absolute risk reduction ΔR ; (b) relative risk reduction $\Delta R/R$

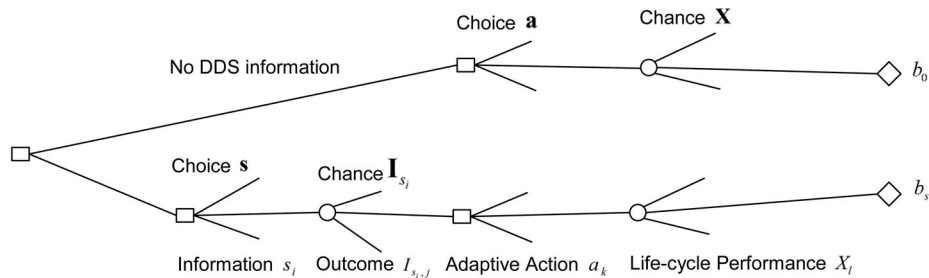


Fig. 9: Decision tree for assessing the value of DDS information (where the rectangles are decision nodes and the circles are chance nodes)

developed in the next section for a case study with a bridge girder system that is subjected to deterioration.

Case Study: Value of the Damage Detection Information for a Pratt Truss Bridge Girder

A statically determinate Pratt truss bridge girder (Fig. 9) is analysed. It is assumed that the girder has been operated for five years without inspection. A further operation until the end of the service life T_{SL} of fifty years is intended. There are indications that the bridge may undergo an abnormal and very high deterioration. The bridge manager knows that a DDS will deliver more information on the condition of the structure but does not know at which point in time during the service life the condition assessment should be performed. In order to determine an optimal point in time, the bridge manager performs an analysis of the value of the DDS information.

The bridge is assumed to be in two system states—namely in the failure state or the safe state. Failure of the truss is caused by component failure due to non-redundant system characteristics and will lead to the costs C_F . Component failure is caused by extreme loads in combination with the damage development over time. The bridge manager has two options: do nothing (action a_0) or repair (action a_1), which will cost C_R . Repair is modelled here as full reconditioning and it is assumed that all damaged components are exchanged.

The probability of system failure $P(F_S)$ can be calculated with a series system formulation with annual (year j) damage increments $\Delta_{D,i,j}$. The initial resistance is reduced by the square of the resistance reduction, which can be shown to be proportional to a

corrosion-induced diameter and consequently section loss. The section loss is also directly proportional to the stiffness loss, for which the probability of indication is determined.

$$P(F_S) = P\left(\bigcup_{i=1}^{n_c=29} M_{R,i} R_{i,0} \times \left(1 - \sum_j \Delta_{D,j}\right)^2 - M_S S_i \leq 0\right) \quad (28)$$

The static, dynamic and structural reliability models of the Pratt truss bridge girder are summarized in Tables 2 and 4. The annual deterioration has been assessed and $\Delta_{D,i,j}$ is assumed to follow a Lognormal distribution with a mean of 0.001 and a standard deviation of 0.001. The mean of the resistance $R_{i,0}$ is calibrated to a probability of $1 \cdot 10^{-6}$, disregarding any damage and considering that the consequence of failure is large and the relative cost of safety measures is small.^{1,47} The probabilistic annual extreme loading S is applied vertically on the truss and evenly distributed on the lower nodes 2, 3, 4, 5, 6, 7 and 8 with $S_i = 1/7 \cdot S$.

The cumulative probability of system failure with time with and changes of the damage and resistance correlation coefficient is shown in Fig. 10. For a constant coefficient of correlation, the probability of system failure increases with time due to the accumulated deterioration damage. When varying the coefficient of correlation from 0.1 through 0.5 to 0.9, the results indicate that with an increase in the coefficient of correlation, the probability of system failure decreases.

The DDS is modelled with acceleration sensors located at nodes 12, 13 and 14 of the truss in the vertical direction to record the response using the sub-space-based DDA (Fig. 11). The

Parameter	Value
Mass per component	0.02
Young's modulus E	14400
Cross-section A	10/144
Length of non-diagonal element	10
Length of diagonal element	$10\sqrt{2}$
Damping ratio	2%

Table 4: Structural model properties

probabilities of indication and the probability of truss system failure given the DDS information of no-indication are calculated following the method laid out previously. The individual probabilities and an exemplary joint probability of indication are shown in Fig. 12. A DDS employment causes costs of C_{DDS} and may cause also damage localization costs C_{loc} in case damage is indicated.

In Fig. 13, the effect of updating the structural system reliability is shown for one DDS utilization (see Eq. (18)) for the different considered damage failure correlations and for different DDS employment years.

The decision analysis for the quantification of the value of the DDS information V is presented in Fig. 14, based on the formulation laid out earlier in the paper. The analysis

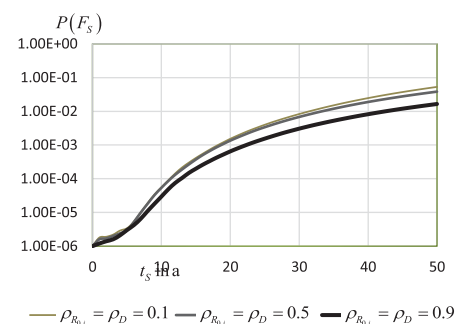


Fig. 10: Probability of system failure over time with varied values of $\rho_{R_{0,i}} = \rho_D = 0.1, 0.5, 0.9$

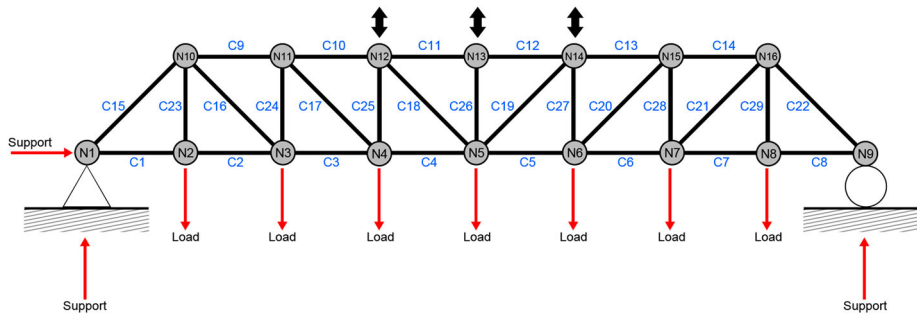


Fig. 11: Pratt truss bridge girder with a distributed load (arrows) and the sensor locations (double arrows)

encompasses the basic decision of whether or not to employ a DDS for condition assessment, the DSS strategies, their outcomes, the actions and the system service life performance, as well as the associated consequences for each branch of the decision tree.

The cost model based on Refs. [48, 49] is shown in Table 5. All costs are discounted with a discount rate of 0.02. During the service life of the bridge, a target system failure probability of $1 \cdot 10^{-4}$ is required, as the costs for safety measures are high and the

consequences remain high.^{1, 47} The cost of repair C_R increases with time due to the damage accumulation and is modelled dependent on the investment cost C_I and the service life T_{SL} (Eq. (29)). When the bridge is repaired, it is assumed that all damaged

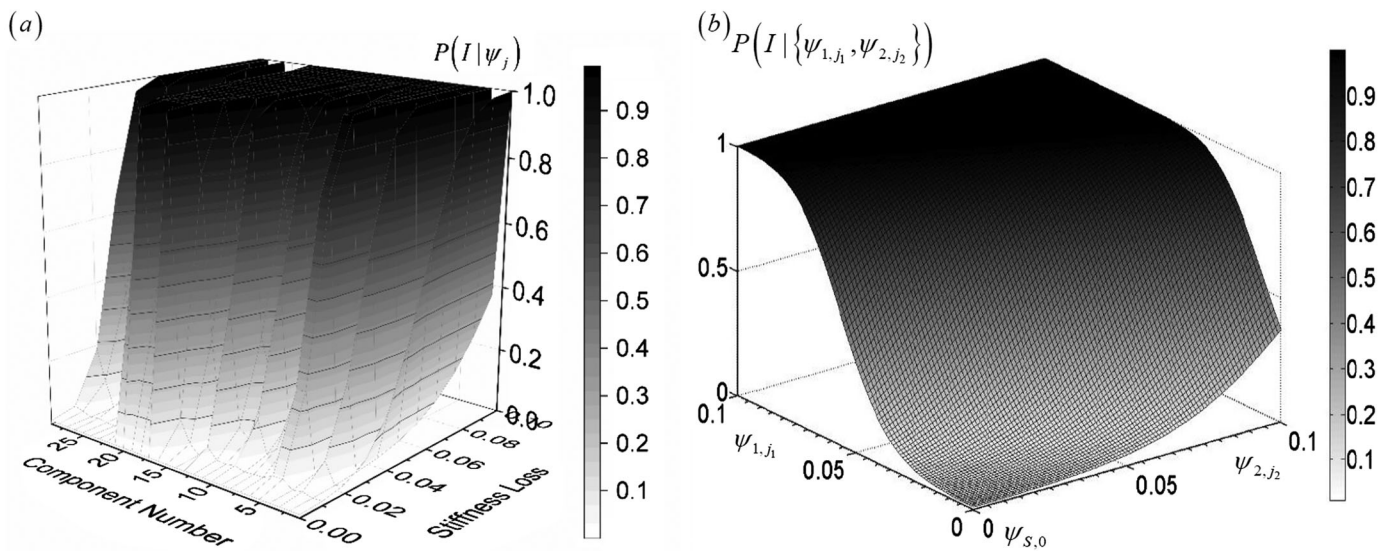


Fig. 12: Probabilities of: (a) indication dependent on the stiffness loss in 29 components; (b) joint probability of indication for components 1 and 2

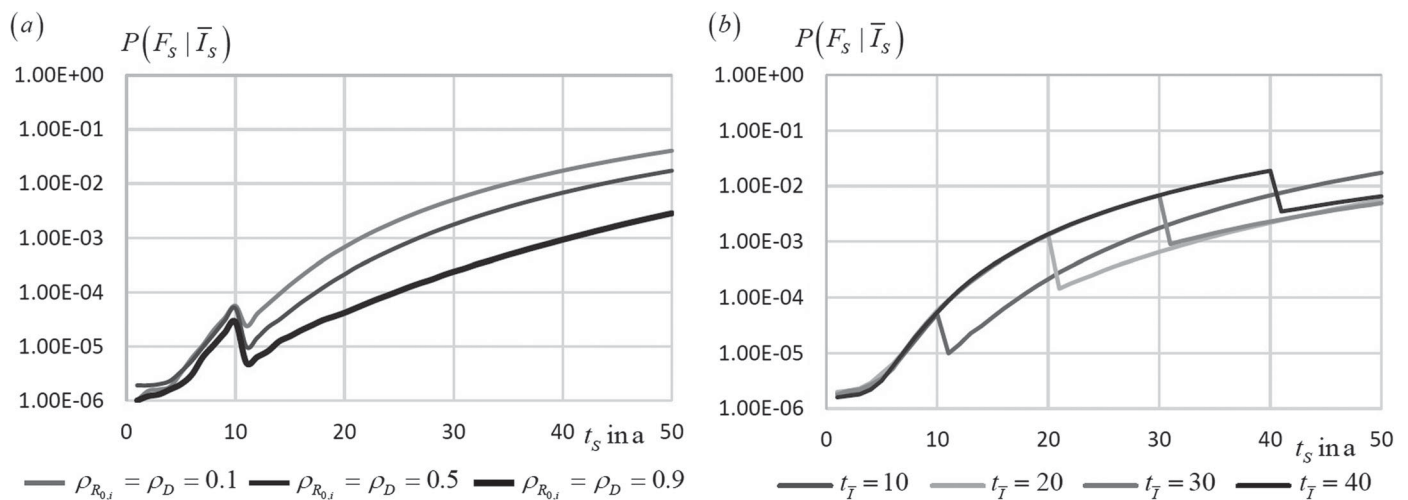


Fig. 13: Posterior probability of system failure: (a) for $P(F_S|\bar{I}_S)$ with varied values of $\rho_{R_{0,i}} = \rho_{D_{0,i}} = 0.1, 0.5, 0.9$ if implementing DDS at year 10; (b) during service life when $\rho_{R_{0,i}} = \rho_{D_{0,i}} = 0.5$ if implementing DDS at year 10, 20, 30 or 40

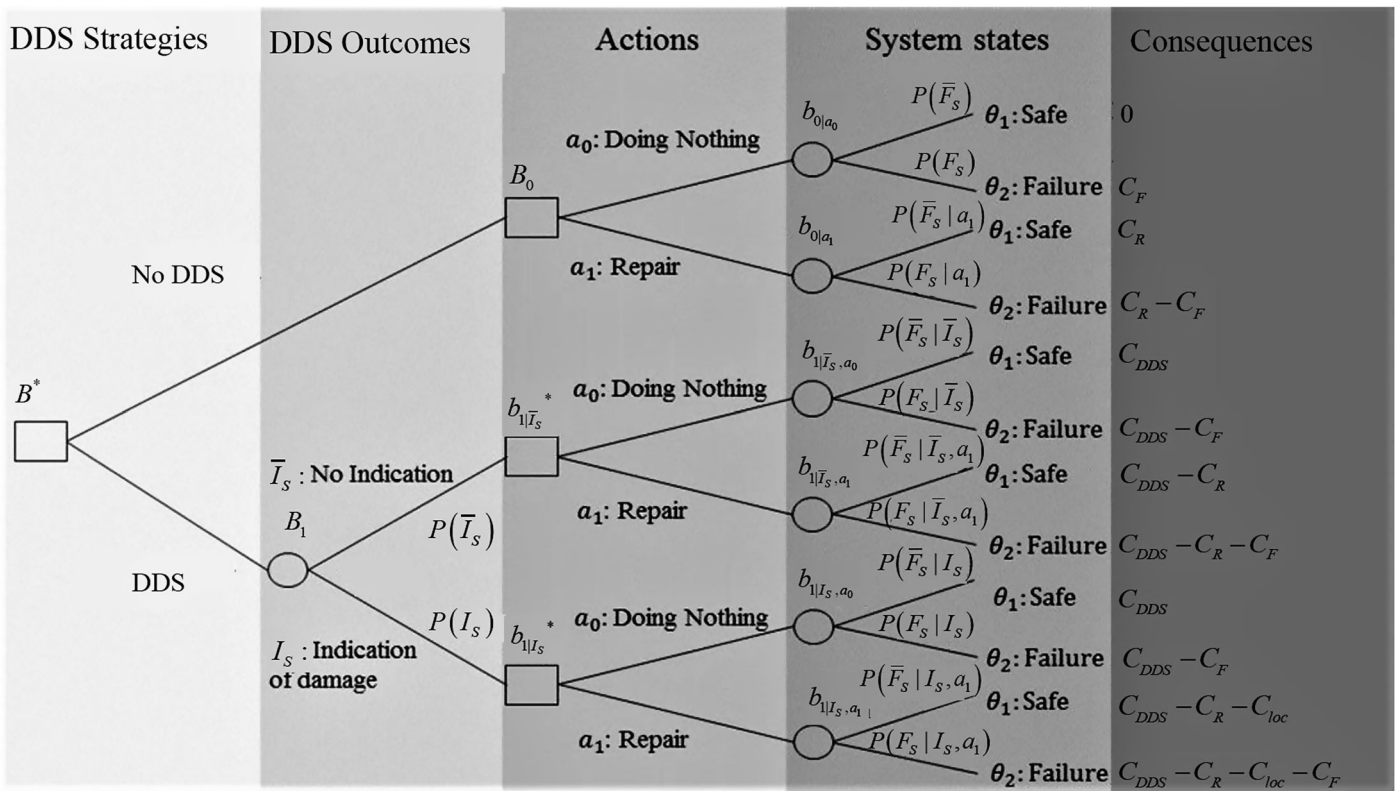


Fig. 14: Decision tree combining a prior decision analysis (branch with no DDS) and a pre-posterior decision analysis to calculate the optimal expected life-cycle benefit B^* for one point in time.

Variable	Discount rate r	Investment cost C_I	Failure cost C_F	Localization cost C_{loc}	DDS cost C_{DDS}
Value	0.02	10	1000	0.1	0.1

Table 5: Parameters in the cost and benefit analysis

components are exchanged with new components:

$$C_R = \frac{C_I}{T_{SL} + 2 - t} \quad (29)$$

The failure cost C_F is assumed to be higher than the investment costs by a

factor of 100 due to indirect consequences. The localization cost C_{loc} and DDS application cost C_{DDS} are assumed equal to 0.1, following for example Ref. [48].

Figure 15 shows the expected costs and risks and the value of the DDS information dependent on the DDS

employment year t_{DDS} . The value of the DDS information is positive between years 7 and 11. The maximum is at year 7, with a significant relative value of the DDS information of 11%. The value of the DDS information is very low in year 6, at which point the DDS information does not influence the repair actions. Only DDS employment in year 7 will lead to changes in the repair actions and hence a reduction in the expected repair costs. The value of the DDS information decreases in the consecutive years, as the period for which the DDS information provides a risk reduction becomes shorter. A drop in the value of

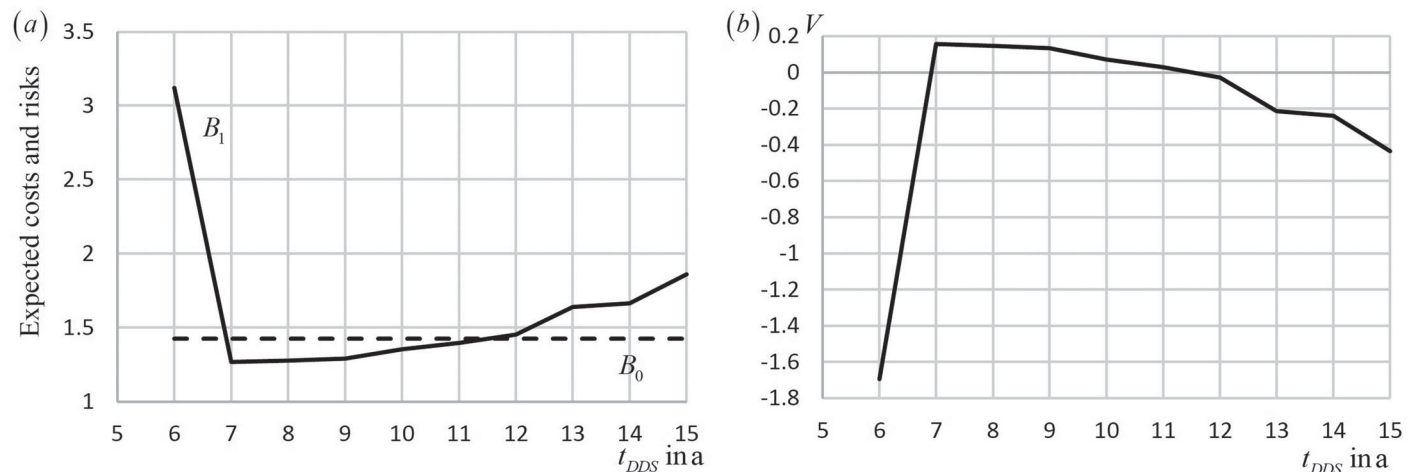


Fig. 15: (a) Expected costs and risks; (b) value of DDS information dependent on the DDS employment year t_{DDS} for $\rho_{R_{0,i}} = \rho_{\Delta_{D,i}} = 0.9$

the DDS information occurs in year 13, as here the optimal action also becomes repair for the branch without the DDS information, as enforced by the target reliability of 10^{-4} .

Conclusions

The introduced approach facilitates the updating of the structural reliability and risks with DDS information at the system level for both the DDS and the structural system. The DDS performance modelling accounts for the characteristics and dependencies of the structural system states and encompasses the measurement system (number of sensors, sensor positions, precision of the system incorporating human errors) and the employed DDAs. The structural system damage states necessitate consistent modelling in terms of the static, dynamic and deterioration characteristics in order to derive the structural reliability and risk, as well as the DDS performance models.

The introduced DDS performance modelling facilitates the comparison and assessment of various DDSs on the basis of the probabilistic indication characteristics at the DDS and structural system levels with for example the system- and/or component-wise and structural system specific probability of indication. The calculation of the DDS performance may demand high experimental or computational resources, as the system damage state space increases exponentially with the number of components. Several strategies to overcome this challenge have been discussed and outlined.

The quantification of the value of the DDS information may serve as a basis for DDS design. In this perspective, a DDS (i.e. the number of sensors, the sensor positions, the precision, the DDA) can be optimized to achieve a maximum expected life-cycle benefit for a specific structural system or class of structural systems.

With two case studies, the potential of the approach has been demonstrated in terms of the significant value of the DDS information and the reduction of the structural system risk by utilizing a subspace-based DDA. The approach is generalizable to other DDAs, requiring the indication characteristics for a

discretization of the system damage state space for a chosen DDA.

Acknowledgements

The COST Action TU1402 on Quantifying the Value of Structural Health Monitoring is gratefully acknowledged for the inspiring discussions, contributions and workshops across the scientific and engineering disciplines with researchers, industrial experts and representatives of infrastructure operators, owners and authorities.

ORCID

Sebastian Thöns  <http://orcid.org/0000-0002-7714-3312>

References

- [1] JCSS, *Probabilistic Model Code*. JCSS Joint Committee on Structural Safety, 2006.
- [2] Thöns S. On the Value of Monitoring Information for the Structural Integrity and Risk Management. *Comput.-Aided Civ. Infr. Eng.* 2018; **33**: 79–94.
- [3] Faber MH, (ed). Risk Assessment in Engineering – Principles, System Representation & Risk Criteria: JCSS Joint Committee on Structural Safety; 2008.
- [4] Farrar CR, Worden K. An introduction to structural health monitoring. *Philos. Trans. Royal Soc. London A: Math., Phys. Eng. Sci.* 2007; **365**(1851): 303–315.
- [5] Farrar CR, Doebling SW, Nix DA. Vibration-based structural damage identification. *Philos. Trans. Royal Soc. London A: Math, Phys Eng. Sci.* 2001; **359**(1778): 131–149.
- [6] Carden EP, Fanning P. Vibration based condition monitoring: a review. *Struct Health Monit.* 2004; **3**(4): 355–377.
- [7] Ditlevsen O, Madsen HO. *Structural Reliability Methods, Coastal, Maritime and Structural Engineering and Department of Mechanical Engineering*. Kgs. Lyngby: Technical University of Denmark, 2005.
- [8] Faber MH, Straub D, Maes MA. A computational framework for risk assessment of RC structures using indicators. *Comput-Aided Civ. Inf. Eng.* 2006; **21**: 216–230.
- [9] Straub D, Kiureghian AD. Reliability acceptance criteria for deteriorating elements of structural systems. *J. Struct. Eng.* 2011; **137**(12): 1573–1582.
- [10] Basseville M, Abdelghani M, Benveniste A. Subspace-based fault detection algorithms for vibration monitoring. *Automatica.* 2000; **36**(1): 101–109.
- [11] Döhler M, Mevel L, Hille F. Subspace-based damage detection under changes in the ambient excitation statistics. *Mech. Syst. Signal Proc.* 2014; **45**(1): 207–224.
- [12] Farrar CR, Worden K. *Structural Health Monitoring: A Machine Learning Perspective*. Chichester: John Wiley & Sons, Inc., 2013.

- [13] Papadimitriou C, Beck JL, and Katfygiotis LS. Updating Robust Reliability Using Structural Test Data. *Probabilistic Eng. Mech.* 2001; **16**(2): 103–113.
- [14] Moan T. *Reliability and risk analysis for design and operations planning of offshore structures*. Structural Safety & Reliability: Rotterdam, 1994.
- [15] Gollwitzer S, Rackwitz R. On the reliability of Daniels systems. *Struct. Saf.* 1990; **7**: 229–243.
- [16] Nishijima K, Maes MA, Goyet J, Faber MH. Constrained optimization of component reliabilities in complex systems. *Struct. Safet.* 2009; **31**: 168–178.
- [17] Baker JW, Schubert M, Faber MH. On the assessment of robustness. *Struct. Saf.* 2008; **30**: 253–267.
- [18] Magalhaes F, Cunha A, Caetano E. Vibration based structural health monitoring of an arch bridge: from automated OMA to damage detection. *Mech. Syst. Signal Proc.* 2012; **28**: 212–228.
- [19] Döhler M, Hille F, Mevel L, Rucker W. Structural health monitoring with statistical methods during progressive damage test of S101 Bridge. *Eng. Struct.* 2014; **69**: 183–193.
- [20] Balmès E, Basseville M, Bourquin F, Mevel L, Nasser H, Treysède F. Merging sensor data from multiple temperature scenarios for vibration monitoring of civil structures. *Struct. Health Monit.* 2008; **7**(2): 129–142.
- [21] Deraemaeker A, Reynders E, De Roeck G, Kullaa J. Vibration-based structural health monitoring using output-only measurements under changing environment. *Mech Syst Signal Proc.* 2008; **22**(1): 34–56.
- [22] Worden K, Manson G, Fieller NRJ. Damage detection using outlier analysis. *J. Sound Vibration.* 2000; **229**(3): 647–667.
- [23] Bernal D. Kalman filter damage detection in the presence of changing process and measurement noise. *Mech Syst Signal Proc.* 2013; **39**(1): 361–371.
- [24] Basseville M, Mevel L, Goursat M. Statistical model-based damage detection and localization: subspace-based residuals and damage-to-noise sensitivity ratios. *J. Sound Vib.* 2004; **275**(3): 769–794.
- [25] Döhler M, Mevel L. Subspace-based fault detection robust to changes in the noise covariances. *Automatica.* 2013; **49**(9): 2734–2743.
- [26] Peeters B, De Roeck G. Reference-based stochastic subspace identification for output-only modal analysis. *Mech. Syst. Signal Proc.* 1999; **13**(6): 855–878.
- [27] Döhler M, Mevel L. Fast multi-order computation of system matrices in subspace-based system identification. *Control Eng. Pract.* 2012; **20**(9): 882–894.
- [28] Yang N. Application of reliability methods to fatigue, quality assurance and maintenance. In *Proceedings of the 6th International Conference of Structural Safety & Reliability*, Schuëller GI, Shinozuka M, Yao JTP (eds.) Balkema: Rotterdam, 1994; 3–18.
- [29] Singh R. Three Decades of NDI Reliability Assessment, 2000.

- [30] Gandossi L, Annis C. *Probability of Detection Curves: Statistical Best-Practices*. Luxembourg: European Commission, Joint Research Centre, Institute for Energy, 2010.
- [31] Wall M, Wedgwood FA, Burch S. *Modelling of NDT reliability (POD) and applying corrections for human factors*. Copenhagen: NDT, 1998.
- [32] Schoefs F, Clément A, Nouy A. Assessment of ROC curves for inspection of random fields. *Struct. Saf.* 2009; **31**: 409–419.
- [33] Lanata F, Schoefs F. Probabilistic assessment of the efficiency of algorithms for crack detection on instrumented RC beams: a non-model based method. *EACS 2012 – 5th European Conference on Structural Control*, Genova, Italy, 2012.
- [34] Thöns S, Döhler M. Structural reliability updating with stochastic subspace damage detection information. *EACS 2012 – 5th European Conference on Structural Control*, Genoa, Italy, 2012.
- [35] Thöns S, Lanata F. Risk and operation optimized damage detection and inspection systems. *11th International Conference on Structural Safety & Reliability (ICOSSAR 2013)*, New York, USA, 2013.
- [36] Döhler M, Thöns S. Efficient Structural System Reliability Updating with Subspace-Based Damage Detection Information. *European Workshop on Structural Health Monitoring (EWSHM)*, Bilbao, Spain, 5–8 July 2016.
- [37] Madsen HO. Model updating in reliability theory. *Proceedings of ICASP 5*, Vancouver, Canada, 1987, 564–577.
- [38] Ayala-Uraga E, Moan T. System reliability issues of offshore structures considering fatigue failure and updating based on inspection. *1st International ASRANet Colloquium*, Glasgow, Scotland, 2002.
- [39] Moan T, Song R. Implications of inspection updating on system fatigue reliability of offshore structures. *J. Offshore Mech Arctic Eng.* 2000; **122**: 173–180.
- [40] Straub D. Reliability updating with inspection and monitoring data in deteriorating reinforced concrete slabs. *11th International Conference on Applications of Statistics and Probability in Civil Engineering (ICASP)*, Zurich, Switzerland, 2011.
- [41] Qin J, Faber MH. Risk management of large RC structures within spatial information system. *Comput-Aided Civ. Infr. Eng.* 2012; **27**: 385–405.
- [42] Lee Y, Song J. System reliability updating of fatigue-induced sequential failures. *J. Struct. Eng.* 2014; **140**: 04013074.
- [43] Schneider R, Fischer J, Bügler M, Nowak M, Thöns S, Borrmann A, Straub D. Assessing and updating the reliability of concrete bridges subjected to spatial deterioration – principles and software implementation. *Struct. Concrete.* 2015; **16**(3): 356–365.
- [44] Thöns S, Schneider R, Faber MH. Quantification of the value of structural health monitoring information for fatigue deteriorating structural systems. *12th International Conference on Applications of Statistics and Probability in Civil Engineering (ICASP12)*, Vancouver, Canada, 2015.
- [45] Hong HP. Reliability analysis with nondestructive inspection. *Struct. Saf.* 1997; **19**: 383–395.
- [46] Thöns S, Faber MH, Rucker W. Optimal design of monitoring systems for risk reduction and operation benefits. *SRESA's International Journal of Life Cycle Reliability and Safety Engineering.* 2014; **3**: 1–10.
- [47] ISO 2394. General Principles on Reliability for Structures ISO 2394, 2015.
- [48] Qin J, Thöns S, Faber MH. On the value of SHM in the context of service life integrity management. *12th International Conference on Applications of Statistics and Probability in Civil Engineering, ICASP12*, Vancouver, Canada, 2015.
- [49] Higuchi S. *Cost-Benefit Based Maintenance Optimization for Deteriorating Structures*. Doctoral dissertation, Fakultät Bauingenieurwesen, Bauhaus-Universität Weimar, Germany, 2007.



IABSE Publications
Digitised Archive
from 1929-1999

Did you know?

IABSE publications between 1929 - 1999 can be downloaded for FREE from the IABSE Archive on the internet - by everyone.

Do full text searches in any part of the papers, or browse by title, author or year.

Explore the Archive with over 80'000 pages and find a treasure of information on research, projects and IABSE.

www.iabse.org/publicationsarchive

PS: Conference Papers published after 1999 are available via Ingenta. Full Papers may be downloaded with a subscription or on a pay per view basis.
www.ingentaconnect.com/content/iabse